

# Robust Satellite Image Transmission over Bandwidth-Constrained Wireless Channels

Yali Wang, Hancheng Lu, Zexue Li, Jian Li

Department of Electronic Engineering & Information Science,

University of Science and Technology of China, Hefei, Anhui 230027 China

ylwang15@mail.ustc.edu.cn, hclu@ustc.edu.cn, lizexue@mail.ustc.edu.cn, lijian9@mail.ustc.edu.cn

**Abstract**—With ability to eliminate the cliff effect and achieve graceful degradation, analog-like transmission such as SoftCast has become a hot research issue for robust image/video delivery over wireless channels. However, it has not been well studied in the case of bandwidth compression, which usually occurs in bandwidth-constrained wireless environments such as satellite communication scenarios. In this paper, we propose an analog-like robust transmission scheme based on Compressive Sensing (CS) for satellite image delivery over bandwidth-constrained wireless channels. The motivation for integration of CS in the proposed scheme lies in the fact that the simple dropping strategy is not optimal for satellite image transmission when bandwidth is insufficient. Considering high information entropy and rich structure information properties of satellite images, we perform an amplitude offset operation and the block-based CS (BCS) procedure to improve the energy efficiency and meet the bandwidth budget respectively. We analyze the system distortion of the proposed scheme and formulate the distortion minimization problem as a resource allocation problem. Then, we propose an efficient two-step strategy to find the optimal solution for bandwidth and power allocation. The simulation results show that the proposed scheme achieves up to 5.5dB gain over the state-of-the-art transmission schemes for satellite image delivery.

**Index Terms**—Analog-like robust transmission, Compressive Sensing, satellite images, bandwidth-constrained wireless channels

## I. INTRODUCTION

With the development of satellite communication technologies, there will emerge numerous mobile satellite applications. Among these applications, image transmissions from satellites to mobile users are required frequently, in the case of transmitting images about urban road congestion conditions, the topography images, a natural disaster scene, etc. However, the existing satellite image transmission systems face many challenges, including a large amount of high-resolution image data, limited bandwidth, fluctuating channel conditions and low computational capabilities. Thus, a robust image transmission scheme over bandwidth-constrained wireless channels is in demand for satellites.

Typically, satellite image transmission systems are designed based on Shannon's separation theorem, which performs source compression and channel coding independently with the preknowledge of Channel State Information (CSI). However, for the satellite image transmission especially in broadcast scenarios, the channels are varying, which may bring about *cliff effect*. That means when the actual channel quality below

a certain threshold, the received quality drops dramatically; while above the threshold, the received quality could not be improved accordingly. Even though many digital schemes [1, 2] are developed to provide robust transmission performance, these new techniques like hierarchical modulation, adaptive modulation and coding, are complex. Because of low computational capabilities of satellites, these schemes are not suitable for satellite image transmission.

Recently, analog-like robust schemes for image/video applications have attracted a lot of attentions [3–6]. These schemes could provide a robust transmission performance over varying wireless channels by analog-like way. In SoftCast [3], 2D/3D Discrete Cosine Transform (DCT) transforms and power allocation techniques for image and video coding are adopted for a graceful degradation performance. Cui *et al.* [4] developed a new bandwidth and power allocation scheme for robust video transmission over rayleigh fading channel. Wu *et al.* [5] proposed a line-based transmission scheme, namely Line-Cast, for high-resolution satellite image broadcast.

Even though many robust analog-like transmission schemes over wireless channels are proposed, the solution to achieve the better performance under the bandwidth-constrained network has not been solved perfectly, especially for satellite images [7, 8]. When the channel bandwidth is insufficient, most of these transmission schemes drop the high frequency bands which carry the least important coefficients to realize bandwidth match. However, this simple discarding strategy might lead to a severe performance degradation for most of the satellite images, especially when the channel bandwidth budget is severely insufficient. Since Satellite images have much structure information which is concentrated in intermediate and high-frequency bands. Apart from this strategy, [8] adopted Shannon-Kotelnikov Mappings (SKMs) to increase the number of chunks that are transmitted over bandwidth-constrained channels. However, the cost incurred is the performance degradation at low Signal to Noise Ratios (SNRs). Besides, [9] developed a structure-preserving Hybrid Digital Analog (HDA) video delivery system, which could achieve better performance in bandwidth-constrained network. However, unlike video content, satellite images have low redundancy and high information entropy, which will cause high bandwidth consumption for HDA transmission.

To tackle the above issue, we develop a robust satellite image transmission scheme over bandwidth-constrained

wireless channels, which is necessary for satellite image transmission. As Compressive Sensing (CS) [10] asserted, a sparse or compressible signal can be reconstructed perfectly with a small number of randomly projected measurements. Meanwhile, many CS image reconstruction algorithms have been developed. In this paper, at the transmitter, we integrate CS into the analog-like transmission scheme to compress the source for reduction of the channel bandwidth requirements. However, CS also poses a critical challenge to analog-like scheme since it makes system distortion hard to formulate. The total distortion in this case is caused by CS sampling and power allocation, which means resource (includes power and bandwidth) allocation are complex.

To overcome the aforementioned challenge, we propose a two-stage resource allocation approach for the proposed scheme to minimize the total distortion. Our main contributions can be described as follows.

1) A satellite image is firstly transformed into several levels with a wavelet transform and each level is further divided into blocks. We integrate block-based CS (BCS) into analog-like scheme to meet bandwidth budget meanwhile provide graceful degradation over varying wireless channels. As for high information entropy of satellite images, we decrease the variance of images wavelet coefficients through an amplitude offset operation to improve energy efficiency.

2) We analyze the system distortion and formulate total distortion in levels. It is hard to formulate distortion in blocks because of the high complexity. Limited to computational capabilities of satellites, we propose an efficient two-stage resource allocation scheme to minimize the total distortion.

3) Various simulations are carried out to evaluate the performance of the proposed scheme under different bandwidth budgets and channel conditions. The simulations demonstrate that the proposed scheme can achieve about 5.5dB gain than baseline schemes.

The rest of this paper is organized as follows. Section II describes the proposed scheme. Section III details the resource allocation approach. Simulation results are presented in Section IV. Finally Section V concludes this paper.

## II. THE FRAMEWORK OF PROPOSED SCHEME

Fig. 1 shows the framework of the proposed robust satellite image transmission scheme. We perform the BCS operation to meet bandwidth budget. Besides, to optimize the system distortion, a two-stage resource allocation scheme is developed for low complexity.

### A. Overview

At the sender side, the satellite image is firstly transformed by multi-level Discrete Wavelet Transform (DWT) and the resulted DWT baseband contains most energy of the image. Therefore, to improve the power efficiency, an amplitude offset operation is performed for the DWT baseband. Besides because of vital importance for image reconstruction, the DWT baseband will be transmitted without CS operation.

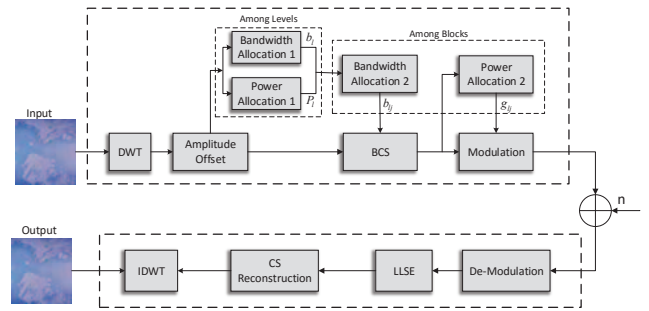


Fig. 1. Framework of the proposed satellite image transmission scheme.

For other levels, the coefficients are divided into blocks. We first perform resource allocation among levels through formulating total distortion, then for low complexity, a further resource allocation among blocks is performed according to CS theory and characteristics of satellite images. Once we get the available bandwidth for each block, BCS operation will be performed to produce measurements. Subsequently, in the analog-like transmission component, the resulted measurements are linearly scaled by the scaling factors derived from the power reallocation. Finally, each two coefficients are mapped to a complex signal through a dense constellation modulation. Besides, to assist the decoding process, some metadata will be transmitted to the receiver side correctly in digital way.

At the receiver side, the received measurements are processed with a Linear Least Square Estimator (LLSE), then a reconstruction component is used to decode CS measurements. Finally, the image is reconstructed through the inverse process component.

### B. Key Components

In this subsection, we will give the details on some key components of the proposed scheme.

1) *Amplitude Offset*: Unlike common natural images, satellite images have high information entropy, low redundancy and rich structure information. At the transform domain of image, most of the energy is concentrated in baseband, so decreasing the variance of baseband coefficients through amplitude offset is necessary for satellite image transmission. It could improve power efficiency significantly. So at wavelet domain, the DWT baseband  $\mathbf{X}_0$  is divided into blocks with size  $c \times d$ , each block is denoted as  $\mathbf{X}_{0j} = [x_{0j}^1, x_{0j}^2, \dots, x_{0j}^m]^T$ , then an amplitude offset operation is performed for each block. The specific implementation is described as follows:

the mean of the  $j$ -th block  $\mathbf{X}_{0j}$  is denoted as

$$\bar{\mathbf{X}}_{0j} = \frac{\sum_{k=1}^m x_{0j}^k}{m}, \quad (1)$$

where the number of coefficients in each block is  $m = c \times d$ . Then the amplitude offset is performed through

$$\mathbf{X}_{0j} = \mathbf{X}_{0j} - \bar{\mathbf{X}}_{0j}. \quad (2)$$

Through the amplitude offset operation, we find that the energy of DWT baseband goes down by an order of magnitude which

improves the power efficiency significantly. It is worth noting that the metadata  $\bar{X}_{0j}$  is transmitted correctly through digital way with strong channel protection.

2) *Compressive Sampling*: For low complexity, the image is divided into blocks and sampled block by block. The linear measurements  $\mathbf{Y}_{lj}$  for each block  $\mathbf{X}_{lj}$  are generated by

$$\mathbf{Y}_{lj} = \mathbf{A}_{lj}\mathbf{X}_{lj}, \quad (3)$$

where  $\mathbf{X}_{lj}$  is the vector of block  $j$  in level  $l$ . Assuming  $b_{lj}$  is the allocated bandwidth for block  $j$ , the number of coefficients in each block is  $n$ , then  $\mathbf{A}_{lj}$  is a  $b_{lj} \times n$  sensing matrix, formed by choosing the first  $b_{lj}$  rows from an  $n \times n$  orthonormalized i.i.d Gaussian matrix  $\Phi$ , where  $\Phi$  is a fixed matrix and could be yielded through orthonormalizing an  $n \times n$  matrix whose entries obey i.i.d standard normal distribution. Thus,  $\Phi$  is shared by sender and receiver as the local information, from which  $\mathbf{A}_{lj}$  can be derived directly.

After the BCS operation for all blocks, power allocation is performed to scale the magnitudes of measurements for robustness transmission in the wireless channel. The scaling factor of measurement block  $\mathbf{Y}_{lj}$  is denoted as  $g_{lj}$ . Through wireless channel, the received signal  $\mathbf{Y}'_{lj}$  is corrupted by noise  $\mathbf{E}_{lj}$ , i.e.

$$\mathbf{Y}'_{lj} = g_{lj} \cdot \mathbf{Y}_{lj} + \mathbf{E}_{lj}, \quad (4)$$

where  $\mathbf{E}_{lj}$  is a zero-mean, i.i.d. gaussian noise vector with variance  $\sigma^2$ .

3) *Decoding*: In the decoder, the LLSE is firstly employed to get the estimated coefficients from the noise:

$$\hat{\mathbf{Y}}_{lj} = \frac{g_{lj}\lambda_{lj}^m}{g_{lj}^2\lambda_{lj}^m + \sigma^2} \cdot \mathbf{Y}'_{lj}, \quad (5)$$

where  $\lambda_{lj}^m = \|\mathbf{Y}_{lj}\|_2^2$  is the variance of  $j$ -th CS block. While for the estimated measurements blocks, a favorable reconstruction algorithm is used to get reconstructed wavelet coefficients  $\hat{\mathbf{X}}_{lj}$  through optimizing the problem:

$$\begin{aligned} \min \quad & \|\hat{\mathbf{X}}_{lj}\|_1 \\ \text{s.t.} \quad & \|\hat{\mathbf{Y}}_{lj} - \mathbf{A}_{lj}\hat{\mathbf{X}}_{lj}\|_2 \leq \sigma, \end{aligned} \quad (6)$$

where  $\sigma^2$  is the noise power that quantifies the uncertainty about the measurements  $\hat{\mathbf{Y}}_{lj}$  in case of the measurements are noisy [11].  $\|\cdot\|_1$  denotes the  $\ell_1$  norm, which depends on the prior assumptions of the signal  $\hat{\mathbf{X}}_{lj}$  that is sparse.

### III. RESOURCE ALLOCATION

In this section, we analyze the system distortion of the proposed scheme and formulate the distortion minimization problem as a resource allocation problem. Moreover, an efficient two-stage strategy is proposed to achieve optimal bandwidth and power allocation.

#### A. Problem Formulation

The goal of the resource allocation is to minimize the system distortion, which is expressed as:

$$D = \sum_{l=0}^L \|\mathbf{X}_l - \hat{\mathbf{X}}_l\|_2^2 = \sum_{l=0}^L \sum_{j=1}^{C_l} \|\mathbf{X}_{lj} - \hat{\mathbf{X}}_{lj}\|_2^2, \quad (7)$$

where  $C_l$  is the number of blocks in level  $l$ . In general,  $D$  should comprise of two components: one component (denoted by  $D^s$ ) is the source distortion caused by the subsampling operation, and another component (denoted by  $D^m$ ) is resulted from the channel distortion.

In here, to minimize  $D^s$ , all of the available bandwidth (i.e., the total number of measurements) should be exhausted. However, increasing the number of measurements means decreasing the average available power for each of them, which will in turn aggravate the channel distortion caused by the attached channel noise. Besides, the aforementioned channel distortion is not only impacted by the total number of measurements, but also depended on the power allocation results. These issues make the bandwidth allocation inevitably coupled with the power allocation.

On the other hand, the above distortion optimization problem is very difficult to handle in block levels directly since the source distortion can only be expressed correctly by fitting distortion model, and we may have many blocks for one image which will cause high complexity.

To tame this problem, we propose a two-stage allocation scheme to solve the problem with low complexity. In the first stage, we allocate the bandwidth (i.e., subsampling rate) and power across de-composition levels in the wavelet domain of satellite image. Then, in the second stage, we allocate the bandwidth and power among blocks at each level.

#### B. Stage One: resource allocation among levels

In this stage, the total bandwidth  $B$  and power  $P$  are allocated among the levels of DWT coefficients.

Since  $D$  is equal to the summation of the distortion of each level, we will firstly analyze the distortion for each level, denoted by  $D_l$  including  $D_l^s$  and  $D_l^m$ . Here we reveal that joint bandwidth-power optimization should be performed to determine both the optimal bandwidth allocation and the optimal power allocation.

As for  $D_l^s$ , we use the same model proposed in [12], which gives:

$$D_l^s = \alpha b_l^\beta + \gamma, \quad (8)$$

where  $b_l$  is the number of the measurements, as well denotes the allocated bandwidth. In practice, the parameters  $\alpha, \beta, \gamma$  of this model are derived by decoding a few sets of measurements for a certain image and calculating the distortion, then use these measurement-distortion data to fit the model and obtain the parameters. Particularly, since the DWT baseband is an independent block without CS operation, we set  $D_0^s = 0$ .

For the level  $l$ , the expected channel distortion is:

$$D_l^c = \mathbb{E}\{\|\mathbf{Y}_l - \hat{\mathbf{Y}}_l\|_2^2\} = \frac{\sigma^2 b_l}{g_l^2}, \quad (9)$$

here  $P_l = g_l^2 \lambda_l^m$ , so the total distortion  $D_l^c$  is:

$$D_l^c = \frac{\sigma^2 b_l}{P_l} \lambda_l^m, \quad (10)$$

where  $\lambda_l^m = \|\mathbf{Y}_l\|_2^2$ . From [13], we know  $D_l^m$  is bounded by the channel distortion:  $D_l^m \leq \kappa D_l^c$ . here  $\kappa$  is a constant

relevant to  $b_l$ , which is very difficult to determine theoretically. To tame these issues, we set  $D_l^m$  as the following, which is found to perform well in our experiments:

$$D_l^m = D_l^c \quad (11)$$

Now based on Eqs. (7)(8) and (11), and note  $D_0^s = 0$ , we have:

$$D = \sum_{l=1}^L D_l^s + \sum_{l=0}^L D_l^c \quad (12)$$

The distortion optimization problem is denoted as:

$$\begin{aligned} \min_{b_l, P_l} \quad & \sum_{l=1}^L (\alpha b_l^\beta + \gamma) + \sum_{l=0}^L \frac{\sigma^2 b_l}{P_l} \lambda_l^m \\ \text{s.t.} \quad & \begin{cases} \sum_{l=1}^L b_l \leq B - b_0 \\ \sum_{l=0}^L P_l \leq P \end{cases} \end{aligned} \quad (13)$$

However, this result is still untractable since  $\lambda_l^m$  is the energy for the measurements  $\mathbf{Y}_l$ , which can't be obtained until we get the measurements for each block. Fortunately, according to [14], when  $\Phi_l$  is an orthonormalized i.i.d Gaussian matrix, the energy of  $\mathbf{X}_l$  seems also to be "subsamped" by the subsampling rate  $\eta_l$ , yielding:

$$\lambda_l^m \approx \eta_l \lambda_l^c \quad (14)$$

Combining with Eq. (14) and  $b_l = \eta_l n_l$ , we could rewrite (13) as:

$$\begin{aligned} \min_{\eta_l, P_l} \quad & \sum_{l=1}^L (\alpha n_l^\beta \eta_l^\beta + \gamma) + \sum_{l=0}^L \frac{\sigma^2 \lambda_l^c}{P_l} \eta_l^2 \\ \text{s.t.} \quad & \begin{cases} \sum_{l=1}^L n_l \eta_l \leq B - b_0 \\ \sum_{l=0}^L P_l \leq P \end{cases} \end{aligned} \quad (15)$$

where all of the other elements are known constants except the variables  $\eta_l$  and  $P_l$ . Besides, we can always have  $\alpha\beta < 0$  and  $\beta < 1$  in practice, given the  $P_l$ , for the variable  $\eta_l$ , the second derivative of the objective function is positive definite, based on which we can prove Eq. (15) is a convex optimization problem that could be expediently solved by the interior point methods. So we could find the solution through iterative algorithm.

### C. Stage Two: resource allocation among blocks

After the stage one, we have the assigned bandwidth and power for each level as  $b_l$  and  $P_l$ , which will be reallocated among the blocks of each level at the allocation stage two. Specifically, we perform the resource allocation for blocks based on the results obtained at the allocation stage one.

It is impossible to perform the resource allocation among blocks like that among levels, since high-resolution satellite images have a large volume of data, and there are many blocks at each level, which cause fitting source distortion for each block is unrealistic. Considering different blocks has different impact on satellite image reconstruction, the block with high information should be allocated more bandwidth. So in order to reduce computational complexity, here based on

compressive sensing theory and block importance, we perform the bandwidth allocation scheme among blocks according to its importance as well as sparsity. The simulation demonstrates that the proposed bandwidth allocation scheme achieves better performance.

We first model the importance of one block by its total coefficients energy and perform bandwidth allocation scheme according to block importance. Additionally, different blocks has different sparsity, which has impact on the CS reconstruction, so it should be taken into account for bandwidth allocation scheme.

For each level, assuming the number of blocks is  $C_l$ , the total coefficients energy of the  $j$ -th block is the variance  $\lambda_{l_j}^c$ , where  $\lambda_{l_j}^c = \|\mathbf{X}_{l_j}\|_2^2$ . Then defining the block weight for each block as:

$$w_{l_j} = \frac{\lambda_{l_j}^c}{\sum_{i=1}^{C_l} \lambda_{l_i}^c}, j = 1, 2, \dots, C_l, \quad (16)$$

So according to this, the initial sampling rate is:

$$\eta_{l_j} = \frac{w_{l_j} b_l}{n}, \quad (17)$$

The initial sampling rate can not ensure  $\eta_{l_j} \leq 1$  for all  $j$ . Assuming the sparsity of each block is denoted as  $K_{l_j}$  which is equal to the number of coefficients above a certain threshold  $\xi$ . According to compressive sensing, the sampling rate of each block should not less than  $\nu_{l_j} = cK_{l_j}/n$  which could provide a basic reconstruction quality. Here,  $c$  is constant, we set  $c = 2$ . Simultaneously, different blocks should have different sampling upper bounds  $\pi_{l_j}$ . Then we modify the solution as follows.

First we adjust  $\eta_{l_j} = \pi_{l_j}$  for the block whose sampling rate  $\eta_{l_j} \geq \pi_{l_j}$ . Finding the collect of  $j$  that  $\eta_{l_j} \geq \pi_{l_j}$ , i.e.  $\Omega = \{j | \eta_{l_j} \geq \pi_{l_j}\}$ . Then we set  $\eta_{l_j} = \pi_{l_j}$  for all  $j \in \Omega$ , and the residual bandwidth  $b_{lr} = b_l - \sum_{j \in \Omega} n \pi_{l_j}$  will be allocated all  $j \notin \Omega$  as follows

$$b_{lr} = \sum_{j \notin \Omega} \frac{n \cdot \eta_{l_j}}{\omega_{l_j}}, \quad (18)$$

then obtain  $\eta_{l_j}$  for all  $j \notin \Omega$ . This process will be repeated until  $\eta_{l_j} \leq \pi_{l_j}$  for all  $j = 1, 2, \dots, C_l$ .

Subsequently, we regulate  $\eta_{l_j} = \nu_{l_j}$  for the block whose sampling rate  $\eta_{l_j} \leq \nu_{l_j}$ . The specific operation is finding the collect of  $j$  that  $\eta_{l_j} \leq \nu_{l_j}$ , i.e.  $\Gamma = \{j | \eta_{l_j} \leq \nu_{l_j}\}$ . Without loss of generality, we assume that the variance of blocks is ordered by amplitude in set  $\Gamma$ , i.e.  $\lambda_1^\Gamma \geq \lambda_i^\Gamma \geq \lambda_m^\Gamma$ , and set  $\eta_{l_j} = \nu_{l_j}$  for blocks with large variance while the blocks with least energy will have  $\eta_{l_j} = 0$  to meet

$$\sum_{j \in \Gamma} n \cdot \eta_{l_j} = \sum_{j \in \Gamma} n \cdot \eta_{l_j}', \quad (19)$$

where  $\eta_{l_j}'$  satisfies

$$\eta_{l_j}' = \begin{cases} \nu_{l_j} & j \leq h \\ 0 & h < j \leq m. \end{cases}$$



Even though this fine tuning will make some blocks whose  $\eta_{lj} = 0$  have to be discarded because of limited bandwidth, it is deserved to guarantee the basic reconstruction quality for more energy coefficients blocks which have rich detail information.

Given the bandwidth  $b_{lj}$  for each block and the BCS operation is performed, the power  $P_l$  in each level will be allocated for each block. According to [3], the power allocation problem can be formulated as:

$$\begin{aligned} \min_{\{g_{lj}\}} \quad & \sigma^2 \sum_{j=1}^{C_l} \frac{b_{lj}}{g_{lj}^2} \\ \text{s.t.} \quad & \sum_{j=1}^{C_l} g_{lj}^2 \lambda_{lj}^m \leq P_l. \end{aligned} \quad (20)$$

Although in this paper different blocks has different numbers of coefficients which is different from equal size block in SoftCast, the optimal scaling factor can be easily derived from the conclusions drawn in [3]. So using the technique of Lagrange multipliers, the optimal scalig factor  $g_{lj}$  for coefficients at block  $j$  is denoted as

$$g_{lj} = \sqrt{\frac{P_l \sqrt{b_{lj}}}{\sqrt{\lambda_{lj}^m} \sum_{i=1}^{C_l} \sqrt{b_{li}} \lambda_{li}^m}}. \quad (21)$$

#### IV. PERFORMANCE EVALUATION

This section evaluates the performance of the proposed scheme through extensive simulations using Matlab 2015b. Several satellite images (see Fig. 2) are used as the test data with a resolution of  $1024 \times 1024$ . These satellite images are from the Aerials volume of the USC-SIPI image database [15]. We use an AWGN channel for simplicity and the channel SNR is unknow at the encoder, the target SNR is 5-20dB. Here, the bandwidth compression ratio  $BwRatio$  is defined as

$$BwRatio = \frac{B_w}{m \times n/2}, \quad (22)$$

where  $B_w$  is the available bandwidth (number of wireless symbols) and  $\frac{m \times n}{2}$  is the bandwidth actually in need. Additionally, we evaluate reconstructed image quality using the Peak Signal-to-Noise Ratio (PSNR) in dB.

##### A. Systems Setup

In the proposed scheme, we use a 3-level DWT with the popular 9/7 biorthogonal wavelets as the sampling-domain transformation and the base layer coefficients are divided into blocks with size  $4 \times 4$  for amplitude offset operation. After that all the coefficients are partitioned into blocks of size  $32 \times 32$ . At the decoder side, a NESTA toolbox [11] is introduced for the CS reconstruction. It is worth noting, the transmitted metadata not only consists of the variance  $\lambda_{lj}^m$  in each block for power allocation same with SoftCast, but also includes the mean  $\bar{X}_{0j}$  of each block in DWT baseband for amplitude offset operation. Through the simulation, they take up about less than 4% of the total bandwidth.

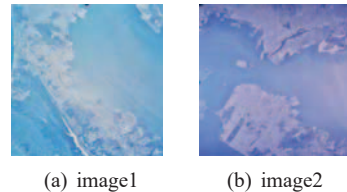


Fig. 2. Test satellite images.

We take SoftCast [3] and SharpCast [9] as reference systems. Even though SharpCast is a HDA video delivery scheme, it also could be used for image transmission over bandwidth-constrained channels. For fair comparison, the size of block is  $32 \times 32$  in SoftCast and SharpCast, other setups are same with original schemes.

##### B. PSNR under Different Bandwidth Budgets

We first evaluate the performance of the proposed scheme and reference systems when channel SNR is 10dB and 15dB. Fig. 3 shows the result of performance comparison under different bandwidth compression ratios. When  $BwRatio < 1$ , the reference schemes discard high frequency bands (the least important blocks) while our proposed scheme uses CS operation to compress source and more blocks could be transmitted. So it can be seen that the proposed scheme performs better than reference schemes with an up to 4.4dB and 5.1dB gain for *image1* and *image2* respectively. Also we can see that more gains are achieved at high bandwidth than low one. The reason is with more measurements, the more blocks are transmitted and the detailed structure is reconstructed well. But there is a certain threshold (*i.e.*,  $BwRatio = 0.7$  for *image1* and *image2*) that when the  $BwRatio$  achieves, the performance gain grows slowly. The reason is that CS reconstruction is performed well for all blocks because of more measurements, and its performance is closed to that condition whose  $BwRatio = 1$ . In addition, the gain of performance not only comes from CS operation but also from the amplitude offset operation for DWT baseband. Seeing the Fig. 3, when  $BwRatio = 1$ , the proposed scheme is same with SoftCast except the amplitude offset operation, and it can achieve about 1.5dB gain for *image1* and *image2* respectively.

##### C. PSNR under Different Channel SNR

In this subsection, we evaluate the performance of the proposed scheme and reference systems under different channel SNR, here the bandwidth compression ratio is set as  $BwRatio = 0.5$  and  $BwRatio = 0.7$ . Under different channel SNRs, which from 5dB to 20dB, the performance of the proposed scheme is shown in Fig. 4. The results show that, our scheme outperforms reference schemes under the same bandwidth budget, with average 3.5dB gains for *image1*, and 4.0dB gains for *image2* when  $BwRatio = 0.7$ , respectively. Here, the gain at high SNR ia larger than that at low SNR because the reconstruction by CS is good enough at high SNR, while the performance of CS recovery is affected badly by noise which causes the smaller gain. Despite this, our scheme

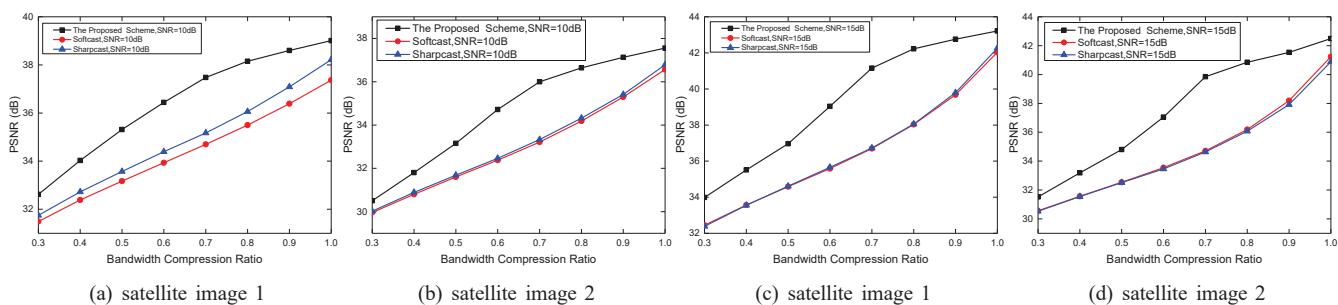


Fig. 3. Performance Comparison under different bandwidth budgets.

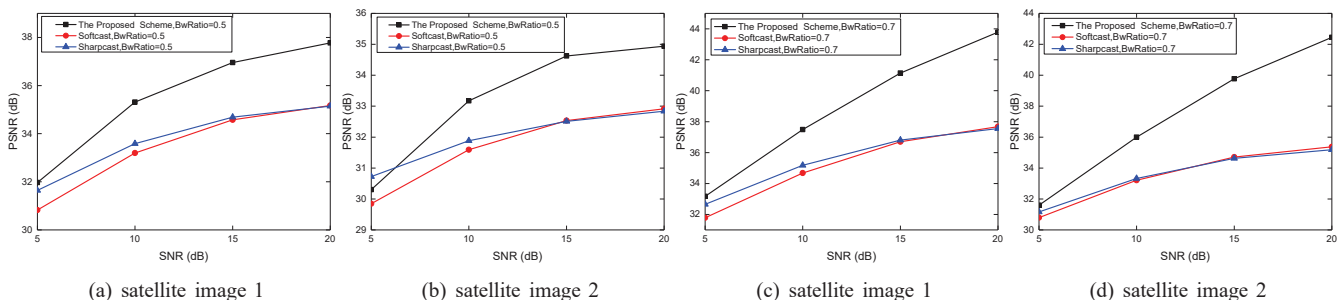


Fig. 4. Performance Comparison under different channel SNR.

achieves graceful degradation and has better performance for satellite image transmission system in bandwidth-constrained wireless networks.

## V. CONCLUSION

In this paper, we propose a robust satellite image transmission scheme for bandwidth-constrained wireless networks. In this work, the amplitude offset for DWT baseband and BCS operation for other levels is performed. Besides, to minimize the total distortion, we implement resource allocation with two steps for low complexity. The simulations show the proposed scheme outperforms the state-of-the-art transmission schemes over bandwidth-constrained wireless channels and provide robust performance.

In the future, we will further explore the robustness of the proposed scheme in wireless fading channels.

## VI. ACKNOWLEDGMENT

This work was supported in part by the National Science Foundation of China (No.61390513, No.91538203) and the Fundamental Research Funds for the Central Universities.

## REFERENCES

- [1] H. Zhou, X. Wang, Z. Liu, X. Zhao, Y. Ji, and S. Yamada, "Qos-aware resource allocation for multicast service over vehicular networks," in *Proc. IEEE WCSP*, 2016, pp. 1–5.
- [2] J. Jin, Y. Ji, B. Zhao, Z. Hao, and Z. Liu, "Error-resilient video multicast with layered hybrid fec/arq over broadband wireless networks," in *Proc. IEEE Globecom*, 2011, pp. 1–6.
- [3] S. Jakubczak and D. Katabi, "A cross-layer design for scalable mobile video," in *Proc. 17th Annu. Int. Conf. Mobile Comput. Netw.*, 2011, pp. 289–300.
- [4] H. Cui, C. Luo, C. W. Chen, and F. Wu, "Robust linear video transmission over rayleigh fading channel," *IEEE Trans. Commun.*, vol. 62, no. 8, pp. 2790–2801, Aug. 2014.
- [5] F. Wu, X. Peng, and J. Xu, "Linecast: line-based distributed coding and transmission for broadcasting satellite images," *IEEE trans. image process.*, vol. 23, no. 3, pp. 1015–1027, Mar. 2014.
- [6] J. Li, X. E. Wen, H. Jia, X. Xie, and W. Gao, "Analogcast: Full linear coding and pseudo analog transmission for satellite remote-sensing images," in *Proc. IEEE Int. Conf. Acoust., Speech and Signal Process.*, 2016, pp. 1362–1366.
- [7] W. Yin, X. Fan, Y. Shi, R. Xiong, and D. Zhao, "Compressive sensing based soft video broadcast using spatial and temporal sparsity," *Mobile Networks and Applications*, pp. 1–11, 2016.
- [8] M. Cagnazzo and M. Kieffer, "Shannon-kotelnikov mappings for softcast-based joint source-channel video coding," in *Proc. Int. Conf. Image Process.*, 2015, pp. 1085–1089.
- [9] D. He, C. Luo, C. Lan, F. Wu, and W. Zeng, "Structure-preserving hybrid digital-analog video delivery in wireless networks," *IEEE Trans. Multimedia.*, vol. 17, no. 9, pp. 1658–1670, Sep. 2015.
- [10] E. J. Candès and M. B. Wakin, "An introduction to compressive sampling," *IEEE signal process. mag.*, vol. 25, no. 2, pp. 21–30, Mar. 2008.
- [11] S. Becker, J. Bobin, and E. J. Candès, "Nesta: a fast and accurate first-order method for sparse recovery," *SIAM J. Imag. Sci.*, vol. 4, no. 1, pp. 1–39, 2009.
- [12] S. Xiang and L. Cai, "Transmission control for compressive sensing video over wireless channel," *IEEE Trans. Wireless Commun.*, vol. 12, no. 3, pp. 1429–1437, Mar. 2013.
- [13] M. A. Davenport, J. N. Laska, J. R. Treichler, and R. G. Baraniuk, "The pros and cons of compressive sensing for wideband signal acquisition: Noise folding versus dynamic range," *IEEE Trans. Signal Process.*, vol. 60, no. 9, pp. 4628–4642, Sep. 2012.
- [14] R. DeVore, G. Petrova, and P. Wojtaszczyk, "Instance-optimality in probability with an  $\ell_1$ -minimization decoder," *Appl. Comp. Harmonic Anal.*, vol. 27, no. 3, pp. 275–288, 2009.
- [15] The USC-SIPI Image Database [Online]. Available: <http://sipi.usc.edu/database/>.